Published December 1, 1992

Okadaic Acid Induces Interphase to Mitotic-like Microtubule Dynamic Instability by Inactivating Rescue

Neal R. Gliksman, Stephen F. Parsons, and E. D. Salmon

Department of Biology, University of North Carolina, Chapel Hill, North Carolina, 27599-3280

Abstract. We used high-resolution video microscopy to visualize microtubule dynamic instability in extracts of interphase sea urchin eggs and to analyze the changes that occur upon addition of 0.8–2.5 μM okadaic acid, an inhibitor of phosphatase 1 and 2A (PP1, PP2a) (Bialojan, D., and A. Takai. 1988. *Biochem. J.* 256:283–290). Microtubule plus-ends in these extracts oscillated between the elongation and shortening phases of dynamic instability at frequencies typical for interphase cells. Switching from elongation to shortening (catastrophe) was frequent, but microtubules persisted and grew long because of frequent switching back to elongation (rescue). Addition of okadaic acid to the extract induced rapid (<5 min) conversion to short, dynamic microtubules typical of mitosis. The frequency of catastrophe doubled and the velocities of elongation and shortening increased slightly; however, the major change was an elimination of rescue. Thus, modulation of the rescue frequency by phosphorylation-dependent mechanisms may be a major regulatory pathway for selectively controlling microtubule dynamics without dramatically changing velocities of microtubule elongation and shortening.

THE conversion from the long, persistent microtubules of interphase into the short, dynamic microtubules of mitosis is controlled by phosphorylation initiated by the activation of maturation promoting factor (MPF) ($p34^{cdc2}$ kinase) (4, 22, 45) and a cascade of downstream kinases, including MAP kinase (15, 16). Addition of either $p34^{cdc2}$ (22, 45) or MAP kinase (16) to interphase cytoplasm or cytoplasmic extracts of *Xenopus* embryos produces conversion to short dynamic microtubules. Conversely, addition of drugs like 6-dimethylaminopurine, an inhibitor of $p34^{cdc2}$ kinase, induces long microtubules when added to mitotic cells (30).

In both interphase and mitotic animal cells, the plus ends of microtubules exhibit dynamic instability, abruptly switching between persistent, constant velocity phases of elongation and shortening (7, 17, 34, 35). Microtubule dynamics and lengths depend on the switching frequencies, catastrophe and rescue, as well as on the velocities of elongation and shortening. Catastrophe and rescue frequencies are difficult to measure accurately because of their stochastic nature, and data must be obtained from measurements of individual microtubules (37, 47). There is now some information on how the parameters of microtubule dynamic instability change between interphase and mitosis (7, 17), and upon activation of $p34^{cdc2}$ kinase in interphase cytoplasm with cyclin B (4). Okadaic acid inhibits the activity of the serine, threonine protein phosphatases 1 and 2a (PP1 and PP2a)[1] (5, 9, 18), and recent studies have shown that treatment with okadaic acid promotes premature and prolonged mitosis in sea urchin eggs (28) and shortens microtubules in interphase tissue culture cells (44). In the experiments reported here, we measured the changes in microtubule dynamics in interphase extracts of sea urchin eggs when phosphorylation was enhanced by inhibiting PP1 and PP2a with okadaic acid.

1. *Abbreviations used in this paper*: PP1 and PP2a, protein phosphatases 1 and 2a.

Materials and Methods

Preparation of Extracts

Interphase extracts from *Lytechinus pictus* (Marinus, Long Beach, CA) eggs were made as previously described (Gliksman, N. R., and E. D. Salmon. 1987. *J. Cell Biol.* 109:30a), from unfertilized eggs, or eggs 15 min after fertilization. Gametes were isolated by intracoelomic injection of 0.56 M KCl. Sperm were collected dry and stored on ice for up to 5 h. Eggs were collected into and washed 3× with artificial sea water (Instant Ocean Aquarium Systems, Mentor, OH). Eggs were then dejellied by washing 2× in isotonic 19:1 (28 mM NaCl, 0.53 mM KCl, 5 mM Tris base, pH 8.0). Egg fertilization was carried out in sea water containing 3-amino-1,2,4-triazole (1 mM) and passed through a 110-μm mesh (Tetko Inc., Elmsford, NY) to remove the fertilization envelopes (36). Unfertilized eggs or eggs 15 min after fertilization were collected in isotonic HEMG buffer (180 mM Hepes, pH 7.35, 10 mM EGTA, 10 mM $MgCl_2$, 0.5 M glycine, 1 mM ATP, 1 mM GTP, 1 mM DTT, and protease inhibitors: 0.3 mM phenyl methyl sulfonyl fluoride, 10 μg/ml p-toluene-sulfonyl-L-arginine methyl ester HCl, 40 μg/ml soybean trypsin inhibitor, 1 μg/ml pepstatin, 1 μg/ml benzamidine HCl, 10 μg/ml aprotinin, and 1 μg/ml leupeptin) and packed with a minimum volume of buffer (20–30% dilution of the cytosol) using a hand centrifuge. The eggs were homogenized and centrifuged at 50,000 *g* for 45 min at 3°C. The clear middle layer was collected with a 25-gauge needle/syringe and used fresh or frozen in liquid nitrogen and stored at −80°C. *L. pictus* egg extracts contained 15–19 μM tubulin (Western blot

Published December 1, 1992

assay) (37, 41) and 20–25 mg/ml total protein (Bio-Rad assay; Bio-Rad Laboratories, Richmond, CA).

Measuring the Dynamic Instability of Microtubules

Microtubules were visualized by video-enhanced differential interference contrast (VE-DIC) microscopy at room temperature (23°C) as previously described (37, 47). Slide preparations were made by diluting the extract samples 4% with HEMG buffer (without protease inhibitors or DTT) containing 0.2 mM ATP, 0.1 mM GTP, 10 μM cytochalasin B, 0–2.5 μM okadaic acid, and salt extracted sea urchin axoneme seeds (47) or sperm centriole complexes (Sluder, G., and F. J. Miller, manuscript in preparation). A 4-μl aliquot of the sample was added to a slide cleaned with ethanol, covered with a biologically clean (23) coverslip (22 × 22 mm, thickness #1), and sealed with valap (a 1:1:1 mixture of Vaseline/lanolin/bees wax) to prevent flowing and drying of the chamber contents.

Perfusion chambers were made from 25 × 25-mm coverslips mounted over two parallel pieces of double-stick tape forming a 70-μm-high by 4-mm-wide channel (43). Perfusion was carried out by adding five chamber volumes of sample to one side of the chamber, and drawing the liquid through with filter paper on the other side. Control experiments showed that perfusion induced no changes in the parameters of dynamic instability of unfertilized interphase egg extract.

Microtubule assembly was videotaped and later analyzed using an IBM-compatible PC-based system for data measurement (47). The standard deviation measured for a stationary object was ± 0.1 μm for repetitive determinations.

Three strategies were used to measure microtubule lengths over time. Straight, nonmotile microtubules were measured by tracking the plus end in real-time or at fixed time intervals (between 0.033 and 2.0 s). Straight, motile microtubules were measured by tracking the two ends of the microtubule independently over the same time interval. The two data sets were combined, and the distance between the two ends was interpolated from the same starting time. Curved microtubules were measured at fixed time intervals (between 0.033 and 2.0 s) by adding up straight lines along the curved microtubule. With all three strategies, velocities of elongation and shortening were calculated from least squares regressions of distance versus time using a minimum of three data points. The catastrophe and rescue frequencies were calculated from the total number of catastrophe or rescue transitions observed, divided by the total length of time spent in either the assembly phase or the shortening phase, respectively (47).

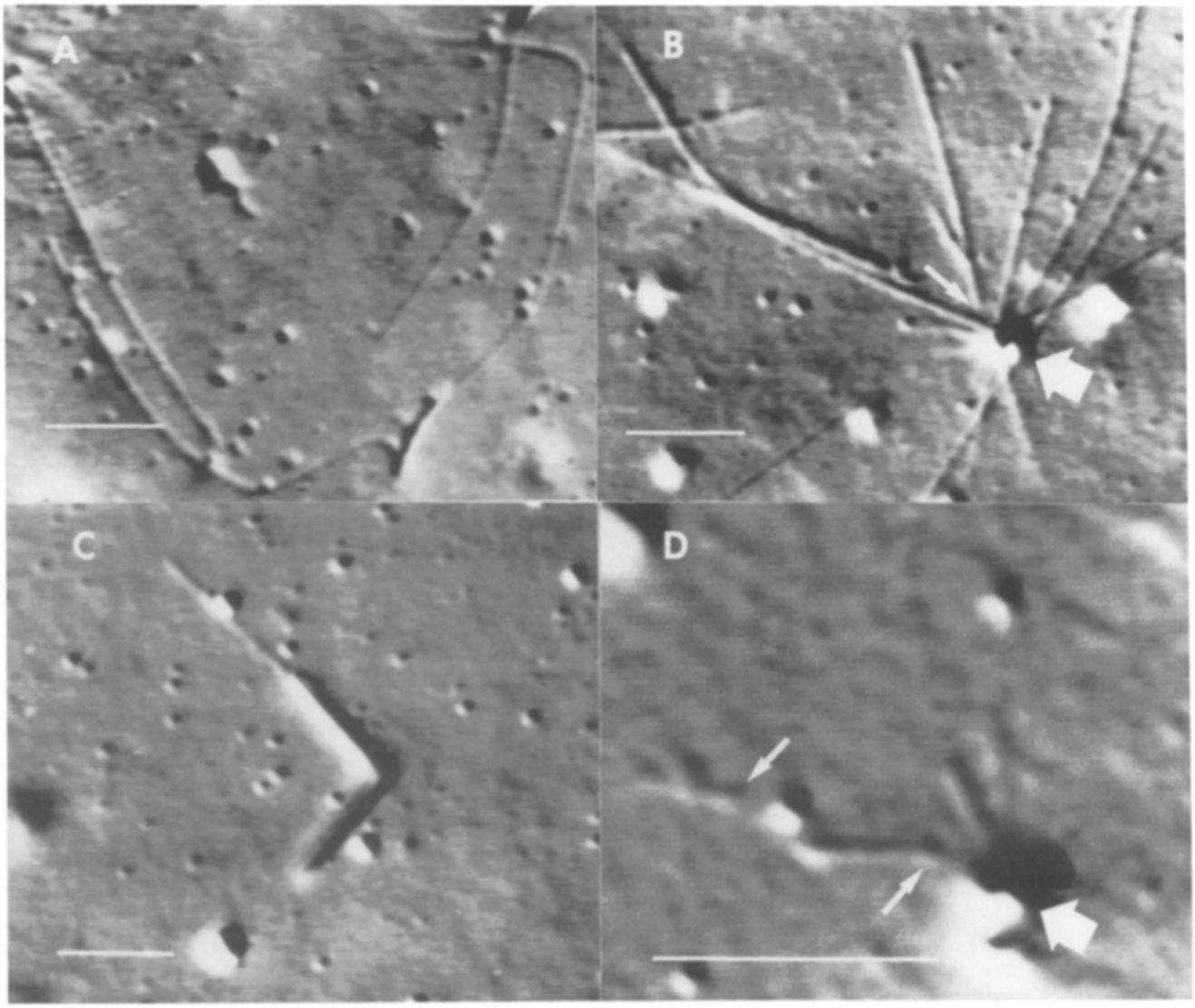

Figure 1. Microtubule assembly in cytoplasmic extracts of *Lytechinus pictus* eggs. Plus-end microtubules assembled in untreated (*A* and *B*) or okadaic acid treated (*C* and *D*) interphase sea urchin egg extracts. Microtubules were nucleated from sperm tail axoneme seeds (*A* and *C*) or sperm centriole complexes (*large arrows* in *B* and *D*). Microtubule motors on the coverslip surface pulled the minus ends of microtubules (*small arrows* in *B* and *D*) from the centriole complexes and translocated microtubules across the coverslip surface away from the nucleating centers. Note that contrast and apparent width of the microtubules and axonemes depend on orientation in VE-DIC. Bars, 5 μm.

Published December 1, 1992

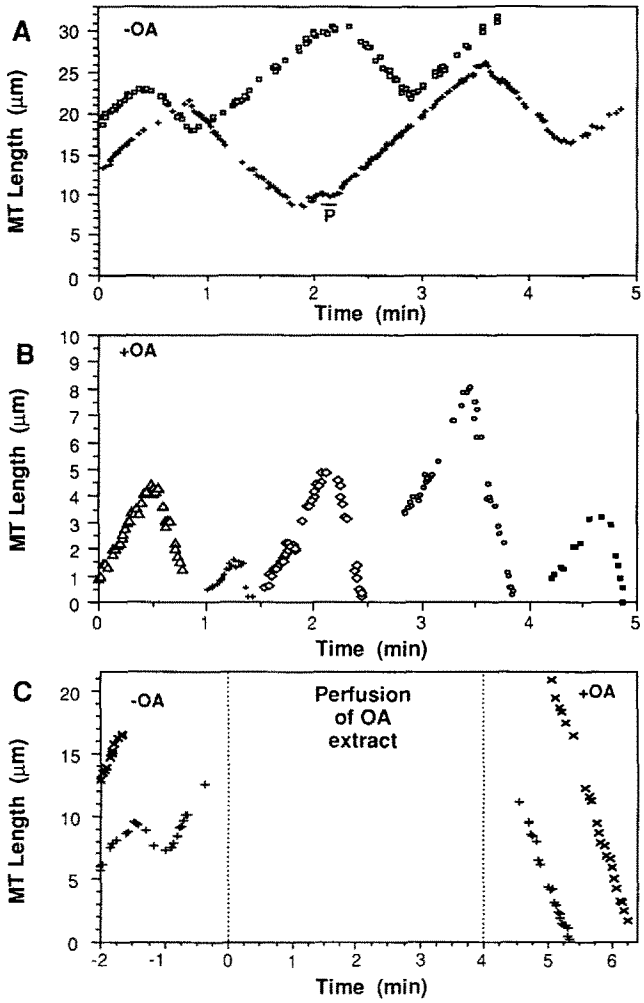

Figure 2. Length histories of microtubules assembled in clarified sea urchin extracts. Different symbols represent different microtubules. (*A*) Microtubule assembly in the interphase extracts was dynamic with rapid elongation, rapid shortening, frequent catastrophes, frequent rescues, and infrequent pauses (*P*). (*B*) Microtubules assembled in okadaic acid–treated extracts displayed rapid elongation, rapid shortening, frequent catastrophes, but no rescues and pauses. (*C*) Perfusion of long microtubules grown in interphase extracts with okadaic acid–pretreated extract rapidly eliminated rescues and pauses. Note the scale changes between *A*, *B*, and *C*.

Measuring the Microtubule Length Distribution

Microtubule length distributions were measured from the same video recordings used to measure microtubule dynamics using the programs described above. Microtubule lengths were measured at each new field of view at time periods between 5 and 6 min after warming the sample. Bundled microtubules and microtubules off of the glass surface were not measured. Since microtubule lengths were limited by the screen dimensions (30–40 μm depending upon the magnification), the lengths of microtubules extending beyond the screen borders were doubled (48). At least 50 microtubules were measured for each histogram.

The Simulation Program

Microtubule dynamic instability was simulated using a Monte Carlo computer program (see ref. 2, and Gliksman, N. R., E. D. Salmon, and R. A. Walker. 1987. *J. Cell Biol.* 111:298a). The program was written in Turbo Pascal V. 5 (Borland International, Scotts Valley, CA) and run on IBM PC compatible computers. The program simulated a population of plus-end microtubules undergoing dynamic instability. The dynamic instability parameters were applied to each plus end in a Monte Carlo fashion at one-second time intervals for a period equivalent to 5 min. All histograms represent the average of 500 ends. All variables were made independent of tubulin concentration, and pauses were ignored for these simulations.

Results and Discussion

We viewed the dynamic instability of individual microtubules in cytoplasmic extracts using high-resolution, VE-DIC light microscopy (7, 37, 47). Concentrated interphase cytoplasmic extracts were made from unfertilized *Lytechinus pictus* eggs or eggs 15 min after fertilization. At pH 7.3, the natural pH of fertilized eggs, little spontaneous self-assembly occurred in the extracts. However, sperm tail axonemal fragments (Fig. 1 *A*) and sperm centriole complexes (Fig. 1 *B*) nucleated plus end (but not minus end) microtubule assembly as previously observed (12, 37, 38, 39). We used low concentrations of nucleation sites (1 or 2 per 35-μm video field) so that microtubule assembly did not significantly deplete the concentration of unpolymerized tubulin in our preparations.

Long, persistent microtubules typical of interphase cytoplasm (7, 34, 35) grew in the egg extracts at 23°C (Figs. 1, *a* and *b*, and 2, *a* and *c*). The rate of plus-end microtubule elongation was 9.1 ± 2.9 μm/min, while the rate of shortening was 12.3 ± 4.4 μm/min (Table I). Elongating ends grew for a mean duration of 53 s and a mean length of 8.0 μm before catastrophe and switching to shortening. Shortening occurred for only 28 s and 5.7 μm on average before rescue back to elongation. Nearly all shortening events were rescued, so that the interphase microtubules did not achieve steady-state lengths. Instead, microtubules persisted and continued to grow longer at a net rate of ~1.7 μm/min.

{net growth rate = [(elongation rate × elongation duration) − (shortening rate × shortening duration)]/(elongation duration + shortening duration)}.

Pauses in microtubule assembly, noted previously both in vivo (34) and in vitro (37, 47), represented only a minute fraction (6–7%) of the observed microtubule lifetimes.

Addition of 0.8–2.5 μM okadaic acid (the predicted concentration of PP1 and PP2a in the sea urchin egg) (9, 28) to the interphase extracts reduced microtubule lengths and lifetimes to the short steady-state values typical of mitosis (1, 33, 45) (Fig. 1 *C*). This conversion in microtubule length and dynamics was not produced by major changes in either the velocities of elongation or shortening; there was little change in the velocity of elongation, and the velocity of shortening increased by <30% (Table I; Fig. 3). Microtubules were much shorter and more labile due to a twofold increase in catastrophe frequency, an elimination of pauses, and a complete inhibition of rescue (Table I; Fig. 3). Rescue was the parameter of dynamic instability most sensitive to okadaic acid. Rescue was undetectable within 5 min of okadaic acid addition and after a catastrophe, microtubules shortened all the way back to the nucleation center. Methyl okadaate and 1-nor okadaone are analogs of okadaic acid which are not phosphatase inhibitors (27). Neither analog inhibited microtubule rescue in our interphase extracts.

Perfusion chambers were also used to determine how quickly rescue was eliminated after okadaic acid treatment for microtubules initially grown to long lengths in untreated extract. We first grew long microtubules in interphase ex-

Published December 1, 1992

Table I. Parameters of Microtubule Dynamic Instability

Extract	OA conc.	Elongation rate ± SD	Shortening rate ± SD	Catastrophe rate*	Rescue rate*
	(μm)	*(μm/min) (N)*	*(μm/min) (N)*	*(Total time) (S^{-1})*	*(Total time) (S^{-1})*
1	0	8.7 ± 1.7 (41)	10.3 ± 4.7 (32)	0.029 (831 s)	0.073 (372 s)
1	1.25	10.1 ± 3.1 (15)	14.6 ± 2.9 (14)	0.051 (215 s)	0.012§ (244 s)
2	0	7.5 ± 1.6 (9)	–	0.020 (256 s)	–
2	1.0	9.9 ± 2.5 (14)	11.5 ± 4.1 (17)	0.057 (192 s)	0.00 (344 s)
3	0	10.8 ± 2.6 (41)	13.8 ± 3.5 (40)	0.017 (1152 s)	0.023 (986 s)
3	2.5	11.3 ± 3.3 (22)	18.4 ± 4.3 (24)	0.026 (352 s)	0.00 (284 s)
4	0	7.8 ± 3.0 (49)	12.7 ± 4.2 (27)	0.016 (1698 s)	0.034 (790 s)
4	2.5	7.2 ± 1.3 (33)	15.9 ± 4.5 (38)	0.034 (841 s)	0.00 (798 s)
Mean‡	0	9.1 ± 2.9 (142)	12.3 ± 4.4 (99)	0.019 (3937 s)	0.036 (2148 s)
Mean‡	1.0–2.5	9.2 ± 3.0 (84)	15.3 ± 4.9 (93)	0.038 (1600 s)	<0.002§ (1670 s)

The parameters of microtubule dynamic instability in sea urchin extracts. Extracts and length measurements were made as described in Figs. 1 and 2, and numbers were recorded from the first 20–25 min after warming the sample to 23°C. No differences in microtubule dynamics were noted between microtubules assembling on the glass surface (attached via microtubule motors) or assembling above the glass surface in solution. No differences in microtubule dynamics were noted between microtubules assembling off of axoneme seeds, or sperm centriole complexes, or between microtubules in simple slide coverslip preparations and in the perfusion chambers. *Total time* the duration of either elongation or shortening measured for each extract; *N* is the number of periods of either elongation or shortening measured for each extract.

* The catastrophe and rescue rates were calculated from the number of transitions observed divided by the total time observed in elongation or shortening.

‡ Combined data from all four extracts.

§ Of the few rescue events seen, all occurred within the first 2 minutes of observation.

tracts from axonemes stuck to the inner coverslip surface of a perfusion chamber (Fig. 2 *C*). After 20 min, the microtubules tethered to the axonemes were perfused with extract which had been preincubated with 2.5 μM okadaic acid for 10 min at room temperature. Within 5 min of perfusion, all microtubule plus ends had switched to shortening. They shortened all the way back to the nucleation center without pause or rescue (Fig. 2 *C*).

Although microtubules in untreated interphase extracts had a net growth of 1.7 μm/min, after 5 min in okadaic acid there was no net growth of microtubules because of the absence of rescue. Instead, an average steady-state length was achieved (Fig. 4). As shown in Fig. 4, the length distributions of microtubules measured in the untreated and okadaic acid–treated extracts were similar to the microtubule length distributions predicted by a Monte Carlo computer simulation of microtubule assembly dynamics, using the mean values for the dynamic instability parameters listed in Table I. In the absence of rescue, the microtubule steady-state length distribution was determined only by the growth velocity and catastrophe frequency. We have neglected the role of microtubule severing activity in this analysis since the severing reported in mitotic *Xenopus* extracts (43) was not seen in our extracts before or after okadaic acid treatment.

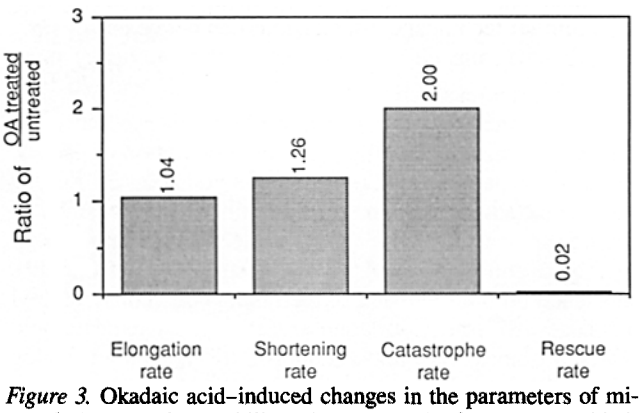

Figure 3. Okadaic acid–induced changes in the parameters of microtubule dynamic instability. The catastrophe frequency doubled, the shortening rate increased slightly, and the rescue frequency decreased substantially when okadaic acid was added to the sea urchin egg extracts. The data was taken from the mean values in Table I.

Nucleation in the cytoplasmic extracts depended both on the type of nucleation center and the treatment history. When axonemes and sperm centriole complexes were added directly to okadaic acid–treated extracts, nucleation from axonemes was infrequent in comparison with the frequency in untreated extracts, but nucleation from the sperm centriole complexes remained robust (Fig. 1, *B* and *D*). This was not surprising since previous studies have shown that axonemal but not centrosomal nucleation is inhibited in meiotic or mitotic cytoplasm in vivo (20). A surprise in the perfusion experiments with okadaic acid–treated extract was the finding that microtubule renucleation occurred almost immediately and was not lost after perfusion (Fig. 2 *B*). Since microtubules were pregrown from the plus ends of axonemes in our perfusion studies, this result suggests that nucleation material in the cytoplasm is recruited to assembled microtubules and transported along the microtubules to the nucleation center (46).

Okadaic acid treatment increased the phosphorylation of a number of extract proteins (seen via SDS-PAGE and autoradiography), and doubled the TCA-precipitable ^{32}P counts, but no phosphorylation of tubulin was detected (data not shown). Comparing the changes in microtubule dynamic instability induced by okadaic acid (Table I and Fig. 3) to those reported to occur upon cyclin B activation of $p34^{cdc2}$ kinase in interphase *Xenopus* extracts (4), we note that neither study found a decrease in elongation or shortening velocities in treated cytoplasm, a result consistent with available in vivo data (7, 17). Our interpretation of the okadaic acid results, along with the microtubule assembly data from *Xenopus* egg extracts treated with cyclin B activated $p34^{cdc2}$ (4) or MAP kinase (14), is that there is a catastrophe factor which is acti-

Published December 1, 1992

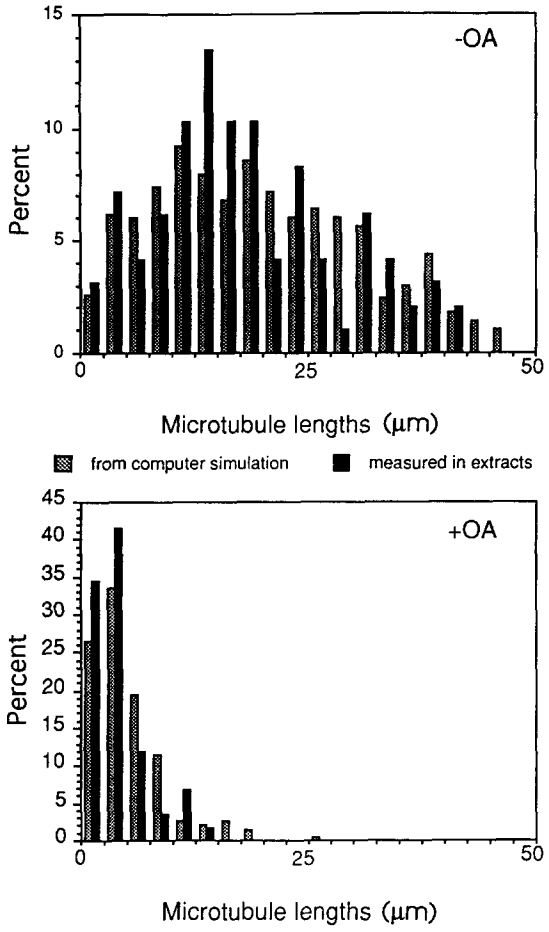

Figure 4. The microtubule length distributions after 5 min of assembly. The distributions show microtubule lengths measured in the extracts as well as microtubule lengths predicted by computer simulation from mean values of the microtubule dynamic instability parameters in Table I. The average microtubule lengths measured in the extracts were 18.2 ± 10 μm (N = 97) and 4.1 ± 2.9 μm (N = 58) for the untreated and okadaic acid-treated samples, respectively. The computer simulations demonstrated that the measured parameters model the assembly of long interphase microtubules typical of untreated extracts, and the short, dynamic, mitotic-like microtubules after okadaic acid treatment. Both sets of simulated microtubules represent 5 min of assembly from 0 length. The parameters for the untreated and okadaic acid-treated extract predicted average microtubule lengths of 18.9 and 4.1 μm after 5 min of simulated assembly. By 15 min, microtubule lengths could not be measured in the interphase extracts because of the video field length (30–40 μm); nevertheless, computer simulations predicted an average microtubule length of 28 μm. After 15 min the microtubules of the okadaic acid-treated extracts remained at a steady-state average length of 4.1 μm.

vated by phosphorylation and a rescue factor which is inactivated by phosphorylation. There is some evidence that these are different molecular complexes (37), but their identities are not yet known.

Okadaic acid, by blocking PP1 and PP2a activity, can enhance the phosphorylation of these presumptive catastrophe and rescue factors in two ways: by directly blocking dephosphorylation of the factors in the presence of a basal level of kinase activity and by activating the kinases which phosphorylate the factors (13, 14, 19, 25, 30, 32, 42). There are a number of kinases which may be responsible for phosphorylation of the catastrophe and rescue factors. Staurosporine (100 μM), an inhibitor of protein kinase C, cAMP kinase, cGMP kinase, pp60$^{c\text{-}src}$, and myosin light chain kinase (24, 40), did not prevent the okadaic acid–induced loss of rescue (data not shown). Although p34^{cdc2} kinase is activated in some cell types by okadaic acid (13, 30, 32), in the sea urchin egg extracts p34^{cdc2} kinase was stimulated only slightly (data not shown). This result is not surprising, since unfertilized eggs and eggs shortly after fertilization contain little of the cyclin A or B needed to activate p34^{cdc2} kinase (11). Okadaic acid has been shown to activate MAP kinase in some cell types (14, 19, 25, 42). In addition, Gotoh et al. (15, 16) have reported that MAP kinase is activated downstream of p34^{cdc2} kinase, producing short mitotic-like microtubules without activating the p34^{cdc2} kinase. Based on this information, we tested whether okadaic acid would induce MAP kinase activation in our sea urchin extracts by measuring the phosphorylation of exogenous MAP2 and MBP, both known substrates for MAP kinase (8, 14, 15, 19, 25, 31, 42). We found that a MAP2 and MBP kinase activity increased two- to threefold in the presence of okadaic acid (data not shown), similar to the increase in this activity at mitosis reported for sea urchins embryos (29). Our data support a role of MAP kinase in the regulation of catastrophe and rescue frequency, but do not preclude the contributions of other unknown kinases.

Cyclin B activated p34^{cdc2} kinase (4) and okadaic acid inhibition of PP1 and PP2a activity both activate MAP kinase and produce similar redistributions of microtubule lengths. For example, compare the microtubule length distributions of Fig. 4 with Fig. 2 of reference 45, Fig. 5 of reference 21, Fig. 3 of reference 16, Fig. 7 *a* of reference 1 and Fig. 6 of reference 6. As a result, we expected them to change the catastrophe and rescue frequencies in the same way. Belmont et al. (4) reported that the short dynamic microtubules in cyclin B–activated extracts were produced by a six- to eightfold increase in catastrophe frequency, with little decrease in rescue frequency. In contrast, we found that okadaic acid treatment produces only a twofold activation of catastrophe, but a total elimination of rescue. Belmont et al. (4) were uncertain of their rescue measurements in the activated extracts because of the high density of short microtubules near the centrosomes. It is possible that the rescues they scored in their activated extracts were not true rescues of a single end, but rather elongating ends passing by adjacent shortening ends. Similar technical considerations can not be used to explain the different changes in catastrophe frequency produced by cyclin B activation of p34^{cdc2} activity and okadaic acid; these differences remain an interesting and important puzzle.

It now seems apparent that catastrophe and rescue frequencies are key phosphorylation-dependent regulators of cytoplasmic microtubule lengths and lifetimes, not the velocity of elongation or shortening of individual microtubules. The results of Belmont et al. (4) demonstrated that increases in catastrophe frequency can cause conversion of long, persistent, interphase microtubules into short, labile, mitotic-like microtubules. Our experiments have shown that elimination of rescue produces the same result. Changes in phosphorylation make substantial changes in the frequencies of catastrophe and rescue without major changes in the velocities of elongation and shortening. These findings do not

fit some of the current models of microtubule dynamic instability of pure tubulin which tightly couple catastrophe and rescue frequencies to the rates of growth and shortening (see for example reference 2). These results also mean that the microtubule-associated proteins and tubulin binding factors which regulate catastrophe and rescue frequency are probably functionally distinct from those which regulate elongation and shortening velocities. Furthermore, one can speculate that regulation of catastrophe and rescue frequencies by phosphorylation controls microtubule assembly dynamics not only as a function of the cell cycle, but also during other cell motility and morphogenic processes.

We thank J. R. Simon for sperm axoneme seeds. We also thank G. Sluder (Worcester Foundation for Experimental Biology), and D. D. Vandré (Ohio State University) for early communication of their data, and E. T. O'Brien, N. Salmon, and K. Bloom for critical reading of this manuscript.

This work was supported by National Institutes of Health grant GM24364.

Received for publication 4 March 1992 and in revised form 6 July 1992.

References

1. Aist, J. R., and C. J. Bayles. 1991. Ultrastructural basis of mitosis in the fungus *Nectria haematococca* (sexual stage of *Fusarium solani*). II Spindles. *Protoplasma.* 161:123–136.
2. Bayley, P. M., M. J. Schilstra, and S. R. Martin. 1989. A simple formulation of microtubule dynamics: quantitative implications of the dynamic instability of microtubule populations *in vivo* and *in vitro*. *J. Cell Sci.* 93:241–254.
3. Bayley, P., M. Schilstra, and S. Martin. 1990. The lateral cap model of microtubule dynamic instability. *J. Cell Sci.* 95:33–48.
4. Belmont, L. D., A. A. Hyman, K. E. Sawin, and T. J. Mitchison. 1990. Real-time visualization of cell cycle dependent changes in microtubule dynamics in cytoplasmic extracts. *Cell.* 62:579–589.
5. Bialojan, D., and A. Takai. 1988. Inhibitory effect of a marine-sponge toxin, okadaic acid, on protein phosphatases. *Biochem. J.* 256:283–290.
6. Cassimeris, L. U., P. Wadsworth, and E. D. Salmon. 1986. Dynamics of microtubule depolymerization in monocytes. *J. Cell Biol.* 102:2023–2032.
7. Cassimeris, L. U., N. K. Pryer, and E. D. Salmon. 1988. Real-time observations of microtubule dynamic instability in living cells. *J. Cell Biol.* 107:2223–2231.
8. Cobb, M. H., T. G. Boulton, and D. J. Robins. 1991. Extracellular signal-regulated kinases: ERKs in progress. *Cell Regul.* 2:965–978.
9. Cohen, P., S. Klumpp, and D. L. Schelling. 1989. An improved procedure for identifying and quantifying protein phosphatases in mammalian tissues. *FEBS (Fed. Eur. Biochem. Soc.) Lett.* 250:596–600.
10. Dunphy, W. G., and J. W. Newport. 1989. Fission yeast p13 blocks mitotic activation and tyrosine dephosphorylation of the *Xenopus* cdc2 protein kinase. *Cell.* 58:181–191.
11. Evans, T., E. T. Rosenthal, J. Youngbloom, D. Distel, and T. Hunt. 1983. Cyclin: a protein specified by maternal mRNA in sea urchin eggs that is destroyed at each cleavage division. *Cell.* 33:389–396.
12. Gard, D. L., and M. Kirschner. 1987. Microtubule assembly in cytoplasmic extracts of *Xenopus* oocytes and eggs. *J. Cell Biol.* 105:2191–2201.
13. Goris, J., J. Hermann, P. Hendrix, R. Ozon, and W. Merevede. 1989. Okadaic acid, a specific protein phosphatase inhibitor, induces maturation and MPF formation in *Xenopus* laevis oocytes. *FEBS (Fed. Eur. Biochem. Soc.) Lett.* 245:91–94.
14. Gotoh, Y., E. Nishida, and H. Sakai. 1990. Okadaic acid activates microtubule-associated protein kinase in quiescent fibroblastic cells. *Eur. J. Biochem.* 193:671–674.
15. Gotoh, Y., K. Moriyama, S. Matsuda, E. Okumura, T. Kishimoto, H. Kawasaki, K. Suzuki, I. Yahara, H. Sakai, and E. Nishida. 1991. *Xenopus* M phase MAP kinase: isolation of its cDNA and activation by MPF. *EMBO (Eur. Mol. Biol. Organ.) J.* 10:2661–2668.
16. Gotoh, Y., E. Nishida, S. Matsuda, N. Shiina, H. Kosaka, K. Shiokawa, T. Akiyama, K. Ohta, and H. Sakai. 1991. *In vitro* effects on microtubule dynamics of purified *Xenopus* M-phase-activated MAP kinase. *Nature (Lond.).* 349:251–254.
17. Hayden, J. H., S. S. Bowser, and C. L. Rieder. 1990. Kinetochores capture astral microtubules during chromosome attachment to the mitotic spindle: direct visualization in live newt lung cells. *J. Cell Biol.* 111:1039–1045.
18. Haystead, T. A. J., A. T. R. Sim, D. Carling, R. C. Honnor, Y. Tsukitani, P. Cohen, and D. G. Hardie. 1989. Effects of the tumor promoter okadaic acid on intracellular protein phosphorylation and metabolism. *Nature (Lond.).* 337:78–81.
19. Haystead, T. A. J., J. E. Weiel, D. W. Litchfield, Y. Tsukitani, E. H. Fischer, and E. G. Krebs. 1990. Okadaic acid mimics the action of insulin in stimulating protein kinase activity in isolated adipocytes. *J. Biol. Chem.* 265:16571–16580.
20. Heideman, S. R., and M. W. Kirschner. 1975. Aster formation in eggs of *Xenopus laevis*: Induction by isolated basal bodies. *J. Cell Biol.* 67:105–117.
21. Kitanishi-Yumura, T., and Y. Fukui. 1987. Reorganization of microtubules during mitosis in *Dictyostelium*: Dissociation from MTOC and selective assembly/disassembly in situ. *Cell Motil.* 8:106–117.
22. Lamb, N. J. C., A. Fernandez, A. Watrin, J.-C., Labbé, and J.-C. Cavadore. 1990. Microinjection of $p34^{cdc2}$ kinase induces marked changes in cell shape, cytoskeletal organization and chromatin structure in mammalian fibroblasts. *Cell.* 60:151–165.
23. Lutz, D. A., and S. Inoué. 1986. Techniques for observing living gametes and embryos. *Methods Cell Biol.* 27:89–110.
24. Mabuchi, I., and H. Takano-Ohmura. 1990. Effects of inhibitors of myosin light chain kinase and other protein kinases on the first cell division of sea urchin eggs. *Dev. Growth & Differ.* 32:549–556.
25. Miyasaka, T., J. Miyasaka, and A. R. Saltiel. 1990. Okadaic acid stimulates the activity of microtubule associated protein kinase in PC-12 pheochromocytoma cells. *Biochem. Biophys. Res. Commun.* 168:1237–1243.
26. Neant, I., M. Charbonneau, and P. Guerrier. 1989. A requirement for protein phosphorylation in regulating the meiotic and mitotic cell cycles in echinoderms. *Dev. Biol.* 132:304–314.
27. Nishiwaki, S., H. Fujiki, M. Suganuma, H. Furuya-Suguri, R. Matsushima, Y. Iida, M. Ojika, K. Yamada, D. Uemura, T. Yasumoto, F. J. Schmitz, and T. Sugimura. 1990. Structure-activity relationship within a series of okadaic acid derivatives. *Carcinogenesis (Eynsham).* 11: 1837–1841.
28. Patel, R., and M. Whitaker. 1991. Okadaic acid suppresses calcium regulation of mitosis onset in sea urchin embryos. *Cell Regul.* 2:391–402.
29. Pelech, S. L., R. M. Tombes, L. Meijer, and E. G. Krebs. 1988. Activation of myelin basic protein kinases during echinoderm oocyte maturation and egg fertilization. *Dev. Biol.* 130:28–36.
30. Picard, A., J. P. Capony, D. L. Brautigan, and M. Doree. 1989. Involvement of protein phosphatases 1 and 2A in the control of M phase-promoting factor activity in starfish. *J. Cell Biol.* 109:3347–3354.
31. Ray, R. B., and T. W. Sturgill. 1987. Rapid stimulation by insulin of a serine/threonine kinase in 3T3-L1 adipocytes that phosphorylates microtubule associated protein 2 *in vitro*. *Proc. Natl. Acad. Sci. USA.* 84:1502–1506.
32. Rime, H., and R. Ozon. 1990. Protein phosphatases are involved in the in vivo activation of histone H1 kinase in mouse oocyte. *Dev. Biol.* 141:115–122.
33. Salmon, E. D., R. J. Leslie, W. M. Saxton, M. L. Karow, and J. R. McIntosh. 1984. Spindle microtubule dynamics in sea urchin embryos: analysis using a fluorescein-labeled tubulin and measurements of fluorescence redistribution after laser photobleaching. *J. Cell Biol.* 99:2165–2174.
34. Sammak, P. J., and G. G. Borisy. 1988. Direct observations of microtubule dynamics in living cells. *Nature (Lond.).* 223:724–726.
35. Schulze, E., and M. Kirschner. 1988. New features of microtubule dynamics in living cells. *Nature (Lond.).* 334:356–359.
36. Showman, R. M., and C. A. Foerder. 1979. Removal of the fertilization membrane of sea urchin embryos employing aminotriazole. *Exp. Cell Res.* 120:253–255.
37. Simon, J. R., S. F. Parsons, and E. D. Salmon. 1992. Buffer composition modulates the dynamic instability of microtubules assembled from sea urchin egg tubulin *in vitro*. *Cell Motil.* 21:1–14.
38. Soltys, B. J., and G. G. Borisy. 1985. Polymerization of tubulin *in vivo*: direct evidence for assembly onto microtubule ends and from centrosomes. *J. Cell Biol.* 100:1682–1689.
39. Suprenant, K. 1991. Unidirectional microtubule assembly in cell-free extracts of *Spisula solidissima* oocytes is regulated by subtle changes in pH. *Cell Motil.* 19:207–220.
40. Tamaoki, T. 1991. Use and specificity of staurosporine, UCN-01, and calphostin C as protein kinase inhibitors. *Meth. Enzym.* 201:340–347.
41. Towbin, H., T. Staelhelin, and J. Gordon. 1979. Electrophoretic transfer of proteins from polyacrylamide gels to nitrocellulose sheets: Procedure and some applications. *Proc. Natl. Acad. Sci. USA.* 76:4350–4354.
42. Tsao, H., and L. Greene. 1991. The roles of macromolecular synthesis and phosphorylation in the regulation of a protein kinase activity transiently stimulated by nerve growth factor. *J. Biol. Chem.* 266:12981–12988.
43. Vale, R. D. 1991. Severing of stable microtubules by a mitotically-activated protein in *Xenopus* extracts. *Cell.* 64:827–839.
44. Vandré, D. D., and V. L. Wills. Inhibition of mitosis by okadaic acid: possible involvement of a protein phosphatase 2A in the transition from metaphase to anaphase. *J. Cell Sci.* 101:79–91.
45. Verde, F., J. Labbé, M. Dorée, and E. Karsenti. 1990. Regulation of microtubule dynamics by cdc2 protein kinase in cell-free extracts of *Xenopus* eggs. *Nature (Lond.).* 343:233–343.
46. Verde, F., J.-M. Berrez, C. Antony, and E. Karsenti. 1991. Taxol-induced microtubule asters in mitotic extracts of *Xenopus* eggs: requirement for phosphorylated factors and cytoplasmic dynein. *J. Cell Biol.* 112:1177–1187.
47. Walker, R. A., E. T. O'Brien, N. K. Pryer, M. Soboeiro, W. A. Voter, H. P. Erickson, and E. D. Salmon. 1988. Dynamic instability of individual microtubules analyzed by video light microscopy: rate constants and transition frequencies. *J. Cell Biol.* 107:1437–1448.
48. Zeeberg, B., R. Reid, and M. Caplow. 1980. Incorporation of radioactive tubulin into microtubules at steady state. *J. Biol. Chem.* 255:9891–9899.